molecular oral microbiology

molecular oral microbiology

Localization and function of the accessory protein Mfa3 in *Porphyromonas gingivalis* Mfa1 fimbriae

Y. Hasegawa[1,2], K. Nagano[2], R. Ikai[1,3], M. Izumigawa[1,3], Y. Yoshida[2], N. Kitai[3], R.J. Lamont[4], Y. Murakami[1] and F. Yoshimura[2]

1 Department of Oral Microbiology, Asahi University School of Dentistry, Mizuho, Gifu, Japan
2 Department of Microbiology, School of Dentistry, Aichi Gakuin University, Chikusa-ku, Nagoya, Aichi, Japan
3 Department of Orthodontics, Asahi University School of Dentistry, Mizuho, Gifu, Japan
4 Center for Oral Health and Systemic Disease, School of Dentistry, University of Louisville, Louisville, KY, USA

Correspondence: Yoshiaki Hasegawa, Department of Oral Microbiology, Asahi University School of Dentistry, 1851-1 Hozumi, Mizuho, Gifu 501-0296, Japan Tel./fax: +8158 329 1422; E-mail: haseyoshiaki@dent.asahi-u.ac.jp

Keywords: auto-aggregation; biofilm; Mfa1 fimbriae; periodontal disease; PGN0289
Accepted 1 September 2013
DOI: 10.1111/mom.12040

SUMMARY

The fimbriae of *Porphyromonas gingivalis*, the causative agent of periodontitis, have been implicated in various aspects of pathogenicity, such as colonization, adhesion and aggregation. *Porphyromonas gingivalis* ATCC 33277 has two adhesins comprised of the FimA and Mfa1 fimbriae. We characterized the PGN0289 (Mfa3) protein, which is one of the three accessory proteins of Mfa1 fimbriae in *P. gingivalis*. The Mfa3 protein was present in two different sizes, 40 and 43 kDa, in the cell. The 43-kDa and 40-kDa Mfa3 were detected largely in the inner membrane and the outer membrane, respectively. Purified Mfa1 fimbriae contained the 40-kDa Mfa3 alone. Furthermore, the 40-kDa Mfa3 started with the Ala^{44} residue of the deduced amino acid sequence, indicating that the N-terminal region of the nascent protein expressed from the *mfa3* gene is processed in the transport step from the inner membrane into fimbriae. Immuno-electron microscopy revealed that Mfa3 localized at the tip of the fimbrial shaft. Interestingly, deletion of the *mfa3* gene resulted in the absence of other accessory proteins, PGN0290 and PGN0291, in the purified Mfa1 fimbriae, suggesting that Mfa3 is required for integration of PGN0290 and PGN0291 into fimbriae. A double mutant of *mfa3* and *fimA* genes (phenotype Mfa1 plus, FimA minus) showed increased auto-aggregation and biofilm formation similar to a double mutant of *mfa1* and *fimA* genes (phenotype Mfa1$^-$, FimA$^-$). These findings suggest that the tip protein Mfa3 of the Mfa1 fimbriae may function in the integration of accessory proteins and in the colonization of *P. gingivalis*.

INTRODUCTION

Periodontitis is a complex chronic inflammatory disease of the tooth-supporting tissues that leads to tissue damage, degradation of the alveolar bone, and loss of tooth (Pihlstrom *et al.*, 2005). *Porphyromonas gingivalis* is a major pathogen associated with chronic periodontitis. The organism expresses a number of potential virulence factors, including lipopolysaccharide, gingipains and fimbriae (Lamont & Jenkinson, 1998). Gingipains, composed of arginine-specific (RgpA and RgpB) and lysine-specific (Kgp) proteases, are thought to be involved in a wide range of pathological and physiological processes (Imamura

et al., 2003). The type strain of *P. gingivalis* ATCC 33277 has two distinct types of fimbriae composed of fimbrilins, FimA (the *fimA* gene product) and Mfa1 (the *mfa1* gene product), with apparent molecular masses of about 38 and 75 kDa, respectively (Yoshimura *et al.*, 2009). Both types of fimbriae appear to be evolutionarily unique, since no homologues of FimA or Mfa1 have been reported in any other bacteria. Several studies have demonstrated that the roles of FimA and Mfa1 fimbriae are distinct. FimA fimbriae are prominent adhesins that mediate the colonization of periodontal tissues and the invasion of host cells (Lamont & Jenkinson, 2000; Yilmaz *et al.*, 2002; Amano *et al.*, 2004), and induce inflammatory processes in periodontal tissues through a number of mechanisms (Hajishengallis *et al.*, 2008; Amano, 2010). FimA fimbriae promote initial monospecies *P. gingivalis* biofilm formation but exert a restraining regulation on biofilm maturation, whereas Mfa1 have suppressive and regulatory roles during homotypic biofilm development of *P. gingivalis* (Kuboniwa *et al.*, 2009). In community formation between *P. gingivalis* and *Streptococcus gordonii*, an oral commensal species, FimA fimbriae bind to glyceraldehyde-3-phosphate dehydrogenase present on the streptococcal surface (Maeda *et al.*, 2004), while Mfa1 fimbriae engage the streptococcal SspA/B adhesins (Park *et al.*, 2005; Daep *et al.*, 2008).

In many bacteria, the gene encoding the major fimbrilin typically forms a cluster with several additional genes encoding fimbrial minor components or transport machineries (Proft & Baker, 2009). *Porphyromonas gingivalis* ATCC 33277 also has a set of fimbriae-related genes flanking the *fimA* gene (Dickinson *et al.*, 1988; Watanabe *et al.*, 1996; Naito *et al.*, 2008). FimB, the product of the gene immediately downstream of the *fimA* gene, regulates the length and expression of FimA fimbriae (Nagano *et al.*, 2010). The *fimC*, *fimD* and *fimE*, genes downstream of the *fimB* gene, were reported to be accessory proteins, and co-purify with FimA fimbriae, and the products of these three genes may play critical roles in the adhesive activities of FimA fimbriae, suggesting that FimC, FimD and FimE are a putative tip complex that might serve as an adhesin (Nishiyama *et al.*, 2007). In addition, a *fimE* mutant produced FimC and FimD, but neither were present in FimA fimbriae purified from the mutant, suggesting that FimE is required for the assembly of FimC and FimD onto the FimA fiber. Indeed, FimB–E do not appear to be involved in FimA biogenesis and FimA is produced and polymerized to form the fimbrial structure in the *fimC-E* mutants (Nishiyama *et al.*, 2007; Wang *et al.*, 2007).

As for the Mfa1 fimbriae in ATCC 33277, genome analyses have revealed that *mfa1* exists within a gene cluster consisting of five genes, *mfa1*, *mfa2*, *PGN0289*, *PGN0290* and *PGN0291* (Fig. 1A) (Naito *et al.*, 2008). The downstream genes of *mfa1* have a similar genetic structure to the *fimA* locus (*fimA–fimE*). Recently, we have demonstrated that Mfa2, the gene product immediately downstream of *mfa1*, is involved in length regulation and anchoring of the Mfa1 fimbriae (Hasegawa *et al.*, 2009). We have also shown that PGN0289 (Mfa3), PGN0290 and PGN0291 proteins co-purify with Mfa1 fimbriae, and these proteins may associate with Mfa1 fimbriae as accessory proteins (Hasegawa *et al.*, 2009). While there is similarity in the structure and function between the downstream genes of *fimA* and *mfa1*, encoding for accessory proteins, the assembly mechanism, function and localization of the accessory proteins are unclear.

In this study, we have examined the localization and role of Mfa3 in assembly of Mfa1 fimbriae. We show that Mfa3, one of the three accessory proteins of the fimbrial structure, may function in the integration of accessory proteins, and may be involved in autoaggregation and biofilm formation in *P. gingivalis*.

METHODS

Bacterial strains, plasmids and growth conditions

The bacterial strains and plasmids used in this study are shown in Table 1. All *P. gingivalis* strains were cultivated on Brucella HK agar (Kyokuto Pharmaceutical Industrial, Tokyo, Japan) supplemented with 5% [volume/volume (v/v)] laked rabbit blood, 2.5 μg ml^{-1} hemin, 5 μg ml^{-1} menadione and 0.1 μg ml^{-1} dithiothreitol (DTT) at 37°C for 7 days under anaerobic conditions. Liquid cultures of *P. gingivalis* were in trypticase soy broth supplemented with 0.25% [weight/volume (w/v)] yeast extract, 2.5 μg ml^{-1} hemin, 5 μg ml^{-1} menadione and 0.1 μg ml^{-1} DTT (sTSB). When necessary, 5 μg ml^{-1} chloramphenicol, 20 μg ml^{-1} erythromycin or 1 μg ml^{-1} tetracycline were added to the medium. *Escherichia coli* was

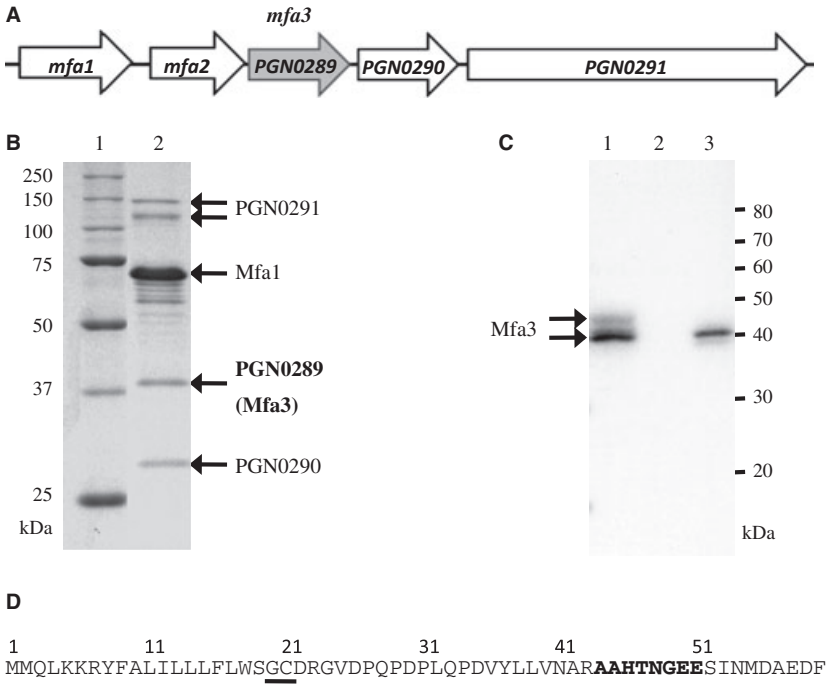

Figure 1 PGN0289 (Mfa3) is an accessory protein of Mfa1 fimbriae. (A) Schematic diagram of the *mfa1* gene cluster in *Porphyromonas gingivalis* ATCC 33277 based on the sequence obtained from NCBI (NC_010729) (Naito *et al.*, 2008). Five genes with the same transcriptional direction were found at this locus (*mfa1-PGN0291*). (B) sodium dodecyl sulfate–polyacrylamide gel electrophoresis (SDS–PAGE) and Coomassie brilliant blue (BB) stain of the purified Mfa1 fimbriae: lane 1, molecular mass marker; lane 2, the purified Mfa1 fimbriae from JI-1 (Δ*fimA*). Previous study showed that PGN0289 (Mfa3), PGN0290 and PGN0291 were accessory proteins of Mfa1 fimbriae (Hasegawa *et al.*, 2009). (C) Western blotting analysis using α-Mfa3: lane 1, the whole cell lysate from JI-1; lane 2, the whole cell lysate from Δ*mfa3* (Δ*mfa3 fimA::erm*); lane 3, the purified Mfa1 fimbriae from JI-1. (D) N-terminal amino acid of Mfa3 in the purified Mfa1 fimbriae from JI-1. The identified amino acid sequence by Edman degradation is indicated in boldface. The N-terminal residue of Mfa3 protein was Ala[44] of the deduced amino acid sequence. The cleavage site for signal peptidase II predicted by LipoP analysis is underlined.

grown in Luria–Bertani medium supplemented, when necessary, with 50 μg ml^{-1} ampicillin, 50 μg ml^{-1} kanamycin or 200 μg ml^{-1} erythromycin.

DNA manipulations

Restriction endonucleases, DNA ligase and related enzymes were purchased from Takara (Otsu, Japan) or New England Biolabs (Ipswich, MA). The oligonucleotides used for polymerase chain reactions (PCR; Table 2) were synthesized by Sigma Genosys (Ishikari, Japan). Standard PCR experiments were performed using a high fidelity DNA polymerase, Pyrobest (Takara), in a PCR Thermal Cycler Dice™ (Takara).

Construction of mutant and complemented strain

We applied the PCR-based overlap extension method (Nagano *et al.*, 2007) to construct DNA fragments that allowed the replacement of *mfa3* gene with the chloramphenicol acetyltransferase (*cat*) gene in the *P. gingivalis* chromosome. The primers are shown in Table 2. The *cat* gene was amplified from the ATG start codon to the TAA stop codon with primers AGU01 and AGU02 to generate a 660-base-pair product from pKD260 plasmid. For construction of the *mfa3*-deletion cassette, the flanking sequence upstream of *mfa3* was amplified with primers Mfa3F1 and Mfa3R1, which have homology to the 5′ end of the *cat* fragment. The flanking sequence downstream of *mfa3* was amplified with Mfa3F2 and Mfa3R2, which have homology to the 3′ end of the *cat* fragment. The *cat*, *mfa3*-upstream and *mfa3*-downstream fragments were used as templates for overlap extension PCR to generate a deletion cassette in which *mfa3* was replaced by *cat*. The PCR product was ligated into a pCR-BluntII-TOPO plasmid vector and the resulting plasmid was introduced into host *E. coli* TOP10 according to the manufacturer's directions (Invitrogen, Carlsbad, CA). Electroporation of

Table 1 Bacterial strains and plasmids used

Strain or plasmid	Genotype and relevant description	Source or reference
Porphyromonas gingivalis		
ATCC 33277	Type strain, Gm^r	ATCC
KDP98	*fimA*-insertional mutant from ATCC 33277, Em^r	Watanabe-Kato *et al.* (1998)
JI-1	*fimA*-deletion mutant from ATCC 33277, Cm^r	Hasegawa *et al.* (2009)
Δ*mfa3*	*mfa3*-deletion mutant from KDP98, Cm^r Em^r	This study
c*mfa3*	Δ*mfa3* carrying pTCOW::*ragAP*::*mfa3*, Cm^r Em^r Tc^r	This study
SMF1	*mfa1*-insertional mutant from ATCC 33277, Em^r	Park *et al.* (2005)
SMF-fimA	*fimA*-deletion mutant from SFM1, Cm^r Em^r	This study
Escherichia coli		
TOP10	F^- *mcrA* Δ (*mrr-hsdRMS-mcrBC*) ω80*lacZ* ΔM15 Δ*lacX74 recA1 araD139* Δ (*ara-leu*)*7697 galU galK rpsL* (Str^r) *endA1 nupG*	Invitrogen
BL21(DE3)	F^- *ompT* $hsdS_B$ (rb-, mb-) *gal dcm rne131* (DE3)	Invitrogen
S17-1	Used for mobilizing pT-COW to *Bacteroides* and *P. gingivalis* via conjugation	Gardner *et al.* (1996)
Plasmids		
pKD260	Plasmid used for a drug cassette, *cat*, Cm^r	Nagano *et al.* (2007)
pCR-Blunt II-TOPO	Cloning vector, Km^r	Invitrogen
pTCOW::*ragAP*	A pTCOW derivative containing a *ragA* promoter region; Ap^r in *E. coli*, Tc^r in *P. gingivalis*	Nagano *et al.* (2012)
pTCOW::*ragAP*::*mfa3*	A pTCOW::*ragAP* derivative containing *mfa3* ORF; Ap^r in *E. coli*, Tc^r in *P. gingivalis*	This study
pET-28	Expression vector, Km^r	Merck
pET-28::*mfa3*	A pET-28 derivative containing *mfa3* ORF; Km^r in *E. coli*	This study
pET-28::*PGN0290*	A pET-28 derivative containing *PGN0290* ORF; Km^r in *E. coli*	This study
pET-28::*PGN0291*	A pET-28 derivative containing *PGN0291* ORF from 1,335 amino acid residue to stop codon; Km^r in *E. coli*	This study

ATCC, American Type Culture Collection; Apr, ampicillin resistance; Cmr, chloramphenicol resistance; Emr, erythromycin resistance; Gmr, gentamicin resistance; Kmr, kanamycin resistance; Tcr, tetracycline resistance.

P. gingivalis was performed essentially as described by Fletcher *et al.* (1995). The plasmid construct was linearized by digestion with *Not*I and *Spe*I and introduced into electrocompetent cells of *P. gingivalis* KDP98 (*fimA*::*erm*) (Watanabe-Kato *et al.*, 1998). After 6 h of anaerobic incubation in sTSB, the pulsed cells were plated on Brucella HK agar supplemented with 5 μg ml^{-1} chloramphenicol, and the plates were incubated anaerobically at 37°C for 7 days. The specific gene replacement was confirmed by PCR and Southern blotting (data not shown).

A complemented strain c*mfa3* was constructed by the introduction of an expression vector, pTCOW::*ragAP*, a pT-COW derivative (Nagano *et al.*, 2007). In brief, the *mfa3* region encoding the putative mature product in ATCC 33277 was amplified by PCR using cMfa3F and cMfa3R with *Xba*I and *Not*I tags, respectively. The resulting fragment was then cloned downstream of the *ragA* promoter region in pTCOW::*ragAP* (Nagano *et al.*, 2012), digested with the appropriate enzymes. The resulting vector pTCOW::*ragAP*::*mfa3* was transferred into *P. gingivalis* Δ*mfa3* via conjugation from *E. coli* S17-1 (Gardner *et al.*, 1996). Expression of Mfa3 protein in c*mfa3* was confirmed by Western blotting (data not shown).

Purification of Mfa1 fimbriae

Purification of Mfa1 fimbriae from *P. gingivalis* was according to our previous protocol (Park *et al.*, 2005; Hasegawa *et al.*, 2009). Briefly, bacterial cells disrupted in a French pressure cell were separated by ultracentrifugation, and then the supernatant was precipitated with ammonium sulfate (50% saturation). The Mfa1 fimbrial fraction was separated by ion exchange chromatography followed by gel filtration chromatography. The degree of purity and identity of Mfa1 fimbriae were verified by sodium dodecyl sulfate–polyacrylamide gel electrophoresis (SDS–PAGE) and mass spectrometry.

Table 2 Primers used in this study

Primer	Sequence (5′–3′)
AGU01	ATGGAGAAAAAAATCACTGGA
AGU02	TTACGCCCCGCCCTGCCACTC
Mfa3F1	GCCTCGAGCAATGGCTCCTATCG
Mfa3R1	CCAGTGATTTTTTTCTCCATATTCCAAGTGTAT ATGGTTA
Mfa3F2	GCAGGGCGGGGCGTAAACAGACTTATGA AAAAGTAT
Mfa3R2	AGATTGTCCGGCTTGGTCGTTGG
cMfa3F	ATACACT**TCTAGA**ATGATGCAGCTTAAAAAGAGAT
cMfa3R	TTTTCAT**GCGGCCGC**CTATTTCTTGATAAA AACTTTAT
rMfa3F	TATACAC**GAATTC**TATGATGCAGCTTAAAAA GAGAT
rMfa3R	TTCATAA**AAGCTT**CTATTTCTTGATAAAAACTTTAT
rPGN0290F	AAATAGA**GGATCC**TATGAAAAAGTATTTGT TATATG
rPGN0290R	GACCTAA**AAGCTT**TCAAATCTCGACTTCGTA CTTGT
rPGN0291F	ACGAGGT**GAATTC**AATGATGAAACGATATAC AATAA
rPGN0291R	TAACATC**CTCGAG**TTACGTCAGATTTTTAACG ATGAAAC

The underlining shows overlapping regions of the 5′ or 3′ end of *cat*. Boldface indicates restriction enzyme sites.

Preparation of recombinant proteins and antisera

To construct a plasmid expressing recombinant Mfa3 protein, the *mfa3* region encoding the putative mature product was amplified by PCR using rMfa3F and rMfa3R with *Eco*RI and *Hin*dIII tags respectively as primers. Chromosomal DNA of ATCC 33277 was used as the template. The resulting fragment was cloned into the expression vector pET-28 (Merck, Darmstadt, Germany), yielding plasmid pET-28::*mfa3* encoding Mfa3. To construct plasmid expressing recombinant PGN0290 protein, the PGN0290 gene region encoding the putative mature product was amplified by PCR using rPGN0290F and rPGN0290R primers with *Bam*HI and *Hin*dIII tags, respectively. For construction of recombinant PGN0291 protein, the N-terminal region of deduced start codon to 1335 amino acid residues was amplified using rPGN0291F and rPGN0291 with *Eco*RI and *Xho*I tags, respectively. The resulting fragments were cloned into the expression vector pET-28, yielding plasmid pET-28::*PGN0290* encoding *PGN0290* gene and pET-28::*PGN0291* gene encoding *PGN0291* gene, respectively. The plasmid was introduced into *E. coli* strain BL21 star (DE3) for overproduction of each protein. The whole cell lysate of transformants was subjected to SDS–PAGE. Strongly expressed protein bands were excised with a clean blade, and the protein in the pieces of the gels was electrophoretically eluted. Identity of the eluted proteins was confirmed by mass spectrometry. Antiserum against Mfa3, PGN0290 or PGN0291 (α-Mfa3, PGN0290 or PGN0291) was prepared. In brief, each recombinant protein was mixed with Freund's complete adjuvant, and was injected into rabbits subcutaneously three times at 2-week intervals. For preparation of anti-Mfa1 fimbriae antiserum (α-Mfa1 fimbriae), purified Mfa1 fimbriae from JI-1 were injected into rabbits as above. Specific antiserum against Mfa1 protein was raised in chickens (Hasegawa *et al.*, 2009). Preparation of antisera was carried out according to the Guidelines for Animal Experiments at the School of Dentistry, Aichi-Gakuin University (AGUD113).

Preparation of cellular fractions

Porphyromonas gingivalis JI-1 was anaerobically cultivated for 24 h, and bacterial cells were washed with 10 mM HEPES-NaOH (pH 7.4) containing 0.15 M NaCl and then resuspended with 10 mM HEPES-NaOH (pH 7.4) containing 0.1 mM *N*-α-*p*-tosyl-L-lysine chloromethyl ketone, 0.2 mM phenylmethylsulfonyl fluoride, and 0.1 mM leupeptin. The cells were disrupted by sonication, and the remaining undisrupted bacterial cells were removed by centrifugation at 1000 ***g*** for 10 min. The supernatant was used as the whole cell lysate. The envelope fraction was collected as a pellet by centrifugation of the whole cell lysate at 100,000 ***g*** for 60 min at 4°C. The supernatant was used as the soluble fraction. The outer and inner membranes were separated by the differential detergent extraction method from envelope fraction with 1% Triton X-100 in HEPES buffer containing 20 mM $MgCl_2$ for 30 min at 20°C (Murakami *et al.*, 2002).

SDS–PAGE and Western blotting

Samples were solubilized in SDS buffer with 2-mercaptoethanol at 100°C for 5 min, then subjected to SDS–PAGE. The gels were stained with Coomassie brilliant blue R-250 (CBB). Proteins in an SDS–polyacrylamide gel were electrophoretically transferred to a PVDF membrane. The membrane was blocked with

5% skim milk in 20 mM Tris–HCl (pH 7.4). Then the membrane was reacted with primary antisera to Mfa3, PGN0290, or PGN0291, followed by incubation with the secondary antiserum, horseradish peroxidase (HRP) -conjugated goat anti-rabbit immunoglobulin G (IgG; MP Biomedicals, Santa Ana, CA) or HRP-conjugated goat anti-chicken IgY (Abcam, San Francisco, CA). After the membrane was washed, signals were detected with ECL-prime (GE Healthcare, Buckinghamshire, UK).

Protein analysis by mass spectrometry

After SDS–PAGE, protein bands were analyzed using matrix-assisted laser desorption ionization–time-of-flight mass spectrometry (MALDI-TOF MS) as described previously (Abe *et al.*, 2011; Kishi *et al.*, 2012). After in-gel tryptic digestion, peptides were extracted, concentrated and analyzed using a 4800 MALDI TOF/TOF Analyzer (Applied Biosystems Biosystems, Foster City, CA). Proteins were identified from the MS peaks using the MS-Fit peptide mass fingerprinting methods in the MASCOT program (http://www.matrixscience.com/).

N-terminal amino acid sequence analysis

N-terminal amino acid sequencing of Mfa3 associated with the purified Mfa1 fimbriae was performed by Edman degradation. The Mfa3 protein in purified Mfa1 fimbriae from *P. gingivalis* JI-1 that had been separated by SDS–PAGE was electrophoretically transferred from the gels onto PVDF membranes. The protein bands of Mfa3 in the membranes were stained with CBB, excised and subjected to N-terminal amino acid sequence analysis by an ABI 477 A automatic peptide sequence analyzer (Center for Instrumental Analysis, Hokkaido University).

Dot immunoblotting

Dot immunoblotting was performed to detect the Mfa3 protein in the purified Mfa1 fimbriae. Nitrocellulose membranes were spotted with 5 μg of the purified Mfa1 fimbriae using a Bio-Dot Microfiltration Apparatus (Bio-Rad, Hercules, CA) and blocked with 10 mM Tris-buffered saline (pH 7.4) containing 0.1% Tween-20 and 5% skim milk. Membranes were then incubated with α-Mfa3 antiserum (1 : 4000) followed by HRP-conjugated goat anti-rabbit IgG before development with ECL-plus kit (GE Healthcare).

Bacterial aggregation

Bacterial aggregation assays using recombinant accessory protein-specific antisera were performed to examine immunoreactivity against native proteins and localization of accessory proteins on the cell surface. JI-1 cells were grown as described above, harvested by centrifugation at 8000 ***g*** for 10 min, gently washed twice with physiological saline, and resuspended in physiological saline. Mfa3, PGN0290 or PGN0291 antisera were added to the cell suspension (1 : 100). The OD_{600} value of each cell suspension was measured at the indicated times at room temperature. All assays were performed in triplicate. α-Mfa1 fimbriae antiserum and pre-immune antiserum were used for positive and negative controls, respectively.

Immunoelectron microscopy

For single immunogold labeling, a drop of bacterial suspension in 10 mM phosphate-buffered saline (PBS; pH 7.4) was placed on nickel grids with formvar carbon support (Okensyoji, Tokyo, Japan), washed three times with PBS and blocked for 1 h in PBS containing 1% bovine serum albumin (BSA). Bacterial cells were stained with primary antiserum (1 : 50 for rabbit α-Mfa1 fimbriae or rabbit α-Mfa3) diluted in PBS containing 1% BSA for 1 h. After washing, samples were treated with 20-nm gold-goat anti-rabbit IgG (EY-lab, San Mateo, CA) diluted 1 : 50 in PBS with 1% BSA for 1 h. For double immunogold labeling, bacterial cells were stained with primary antisera (1 : 50 for chicken α-Mfa1 and 1 : 50 for rabbit α-Mfa3) diluted in PBS containing 1% BSA for 1 h. After washing, samples were treated with 6-nm gold-goat anti-chicken IgG (EY-lab) and 20-nm goat anti-rabbit IgG diluted 1 : 50 in PBS with 1% BSA for 1 h. The samples were finally negatively stained with 1% ammonium molybdate and viewed in a Hitachi H-600 electron microscope (Hitachi, Tokyo, Japan) operating at 100 kV.

Auto-aggregation activity

Cells were grown as described above, harvested by centrifugation at 8000 ***g*** for 10 min, gently washed

twice with 20 mM PBS (pH 6.0) and resuspended in PBS. PBS (pH 6.0) was used throughout the auto-aggregation assays. The optical density at 600 nm (OD_{600}) of the cell suspension was measured and adjusted by dilution with PBS to 1.0. Aliquots (2 ml each) in test tubes (13-mm diameter) were then shaken at room temperature at a speed of 120 strokes min^{-1}. At various time-points, OD_{660} values of the suspensions were measured with a spectrophotometer (mini photo 518R; Taitec, Saitama, Japan).

Biofilm assay

Biofilm formation by *P. gingivalis* was quantified using a microtiter plate assay specifically adapted for *P. gingivalis* (Nagano *et al.*, 2010). Briefly, overnight cultures of *P. gingivalis* were diluted 1 : 20 in sTSB. Aliquots (200 μl) of the diluted samples were anaerobically incubated in the wells of a flat-bottom 96-well polystyrene plate (BD, Franklin Lakes, NJ) for 24 h at 37°C. After discarding the planktonic bacterial cells in the wells, bacterial cells bound to the wells were gently washed three times with 10 mM PBS (pH 7.4), air dried, and then stained with 200 μl of 0.5% (w/v) crystal violet for 15 min. After washing twice with 10 mM PBS (pH 7.4) and then with sterile water to remove excess dye, the cell-bound dye was eluted using 200 μl of 99% ethanol. Biofilm formation was quantified by measuring OD_{595}. Biofilms formed on polystyrene dishes were also evaluated by microscopic observation. Briefly, overnight cultures of *P. gingivalis* were diluted 1 : 20 in sTSB. Aliquots (5 ml) of the diluted samples were anaerobically incubated in a dish (60 mm in diameter, Nunc, Tokyo, Japan) for 24 h at 37°C. The biofilms formed on each dish were washed twice with 10 mM PBS (pH 7.4), stained for 15 min with 0.5% (w/v) crystal violet, and rinsed twice with sterile water. Biofilms were observed under an optical microscope BX41 (Olympus, Tokyo, Japan). JI-1, a mutant deficient in *fimA*, was included as a negative control for biofilm formation.

RESULTS

Mfa3 is an accessory protein of Mfa1 fimbriae

SDS–PAGE stained gels of the purified Mfa1 fimbriae from *P. gingivalis* JI-1 are shown in Fig. 1B. In a previous study we identified the 40-kDa band of the purified Mfa1 fimbriae as PGN0289 (Mfa3) by mass spectrometry (Hasegawa *et al.*, 2009). Here to confirm these observations, Western blotting analysis with α-Mfa3 antiserum was performed. Mfa3 was present at two different sizes of 40 kDa and 43 kDa in the whole cell lysate of *P. gingivalis* JI-1 (Fig. 1C, lane 1), whereas those bands were not detected in the whole cell lysate of *P. gingivalis* Δ*mfa3* (Δ*mfa3 fimA*::*erm*) (Fig. 1C, lane 2). It should be noted that the α-Mfa3 was very specific because none of the bands were detected in the whole cell lysate of Δ*mfa3*. In the purified Mfa1 fimbriae from *P. gingivalis* JI-1 (Fig. 1C, lane 3), PGN0289 was detected at approximately 40 kDa as a single band. The molecular mass of the band of PGN0289 protein in the purified fimbriae completely accorded with our previous report, therefore we concluded that PGN0289 is one of the accessory proteins of the Mfa1 fimbriae. Hence, we named *PGN0289* gene *mfa3*. Although the calculated molecular mass of the Mfa3 protein deduced from the nucleotide sequence is 50046.73 Da, the apparent size of Mfa3 associated with fimbriae is 40 kDa. This discrepancy of molecular mass suggested that the nascent protein expressed from the *mfa3* gene could be processed. Next we performed N-terminal amino acid sequencing of the 40-kDa Mfa3 associated with Mfa1 fimbriae. The N-terminal sequence (AAHTNGEE) was found to start with the Ala^{44} residue of the amino acid sequence deduced from the nucleotide sequence (Fig. 1D).

Detection of a precursor of the Mfa3 protein

The Mfa3 protein is annotated as a membrane protein in the *P. gingivalis* ATCC 33277 database (NC_010729) (Naito *et al.*, 2008). To determine the subcellular localization of the Mfa3 protein, cells of JI-1 were subjected to cellular fractionation as previously described (Murakami *et al.*, 2002), in which whole cell lysate from stationary phase cells was fractionated into envelope and soluble fractions by centrifugation. Then the outer membrane and inner membranes were separated by the differential detergent extraction method from the envelope fraction. The protein samples obtained were blotted with α-Mfa3 antiserum. A representative result is shown in Fig. 2. Mfa3 was detected as the 40-kDa and 43-kDa bands in the whole cell lysate (lane 1). The 40-kDa band was

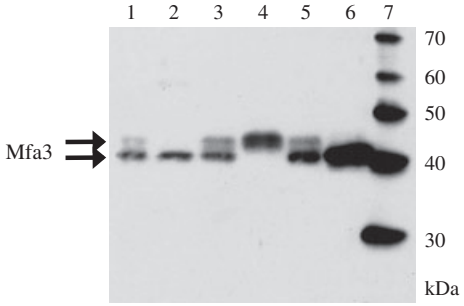

Figure 2 Subcellular localization of Mfa3 protein. Western blots of lysates and subcellular factions of JI-1 with α-Mfa3. Lane 1, whole cell lysate; lane 2, soluble fraction; lane 3, envelope fraction; lane 4, inner membrane fraction; lane 5, outer membrane fraction; lane 6, purified Mfa1 fimbriae; lane 7, molecular mass marker.

clearly detected in the soluble fraction (lane 2). In the envelope fraction both bands were detected (lane 3), and the 43-kDa and 40-kDa bands of the envelope were mainly separated into the inner membrane (lane 4) and the outer membrane fractions (lane 5), respectively. However, the 40-kDa protein alone was present in the purified Mfa1 fimbriae (lane 6), suggesting that the 43-kDa as a precursor was processed and incorporated into filaments of the fimbriae.

Localization of Mfa3 in filaments of the Mfa1 fimbriae

We used immune-electron microscopy with specific antisera including α-Mfa3 to determine the localization of Mfa3 in the fimbrial filaments. First we examined whether the antisera were reactive with the native form of the Mfa1 fimbriae in dot immunoblot analysis and by bacterial aggregation using whole cells. α-Mfa3 strongly reacted with native Mfa1 fimbriae as well as JI-1 cells, but not Δ*mfa3* cells (data not shown). As shown in the Supplementary material (Fig. S1), in the bacterial aggregation assay, α-Mfa3 and α-Mfa1 strongly aggregated intact JI-1 cells, but α-PGN0290 and α-PGN0291 did not aggregate when compared with the OD_{600} curve of pre-immune serum, indicating that α-Mfa3 reacted with epitopes of intact Mfa3, exposed on the surface of Mfa1 fimbriae. However, α-PGN0290 and α-PGN0291 did not recognize intact PGN0290 and PGN0291, respectively, indicating that the reactive epitopes are buried within the molecules.

We carried out immune-electron microscopy using α-Mfa1 or α-Mfa3. As shown in Fig. 3, α-Mfa1 staining

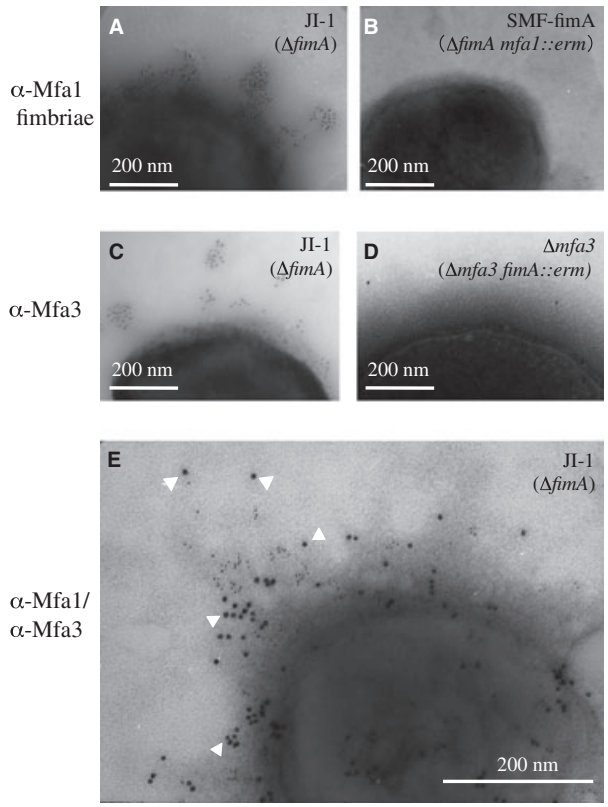

Figure 3 Immune-electron microscopy of Mfa1 fimbriae. Cells of JI-1, SMF-fimA or Δ*mfa3* were labeled with specific antiserum against Mfa1 (rabbit α-Mfa1 fimbriae; A and B) or Mfa3 (rabbit α-Mfa3: C and D) and goat anti-rabbit immunoglobulin G (IgG) conjugated to 20-nm gold particles. For double staining of Mfa1 and Mfa3 proteins, the immobilized JI-1 cells were first reacted with chicken α-Mfa1 and rabbit α-Mfa3 antiserum, followed by incubation with 6-nm gold-labeled anti-chicken IgG and 20-nm gold-labeled anti-rabbit IgG (E). Samples were observed under a transmission electron microscope. Representative images are shown. White arrowheads indicate Mfa3 protein localized at the tip of the fimbrial structure. Scale bars indicate the length of 200 nm.

showed gold particles deposited along filaments around the cell (Fig. 3A), but rarely deposited around the cells without FimA and Mfa1 fimbriae (Fig. 3B). The α-Mfa3-associated gold particles were deposited at positions away from the cell surface (Fig. 3C) when compared with the negative *mfa*3 mutant control (Fig. 3D). Double staining with α-Mfa1 and α-Mfa3 showed the two sizes of gold-particles deposited around the cell in a different fashion, i.e. large particles (indicating Mfa3) were present away from the cell and small particles (indicating Mfa1) were deposited like chains protruding from the cell (Fig. 3E).

PGN0290 and PGN0291 proteins are produced, but not present in the purified Mfa1 fimbriae from Δ*mfa3*

Our previous study reported that the 30-kDa band was identified as PGN0290 and two high molecular weight bands (130-kDa and 150-kDa, respectively) were both identified as PGN0291 in the SDS–PAGE gel of the purified Mfa1 fimbriae (Hasegawa *et al.*, 2009). However, both PGN0290 and PGN0291 were absent in Mfa1 fimbriae purified from Δ*mfa3*, when compared with those from JI-1, as shown in Fig. 4A, although an unknown band appeared at around 50-kDa. Loss of the proteins was confirmed by Western blots (Fig. 4B, C). However, both PGN0290 and PGN0291 were detected in whole cell lysate of Δ*mfa3*, although at lower levels compared with JI-1 (Fig. 5A,B). There are several possible explanations for reduction of PGN0290 and PGN0291 bands in Δ*mfa3*: first, the replacement of *mfa3* gene with the *cat* gene in the chromosome may decrease expression of the downstream gene(s) through a polar effect and, second, PGN0290 and PGN0291 proteins that are unincorporated into fimbriae, could be partially degraded in the cell or released to the culture supernatant. As shown in Fig. 5C, the amount of Mfa1 protein detected in whole cell lysate of Δ*mfa3* was at the same level as JI-1. Mfa1 fimbriae from JI-1 and Δ*mfa3* strains appeared morphologically similar, as shown in Fig. 6A,B.

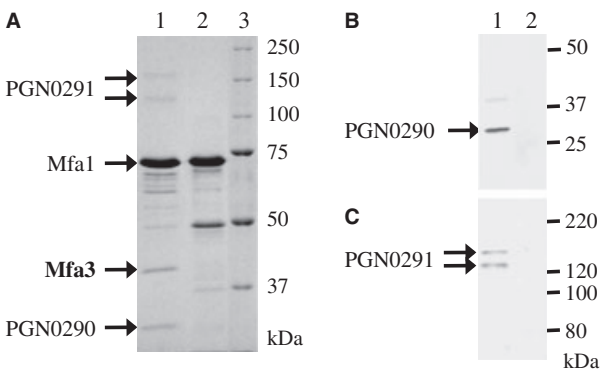

Figure 4 Analysis of the components of purified Mfa1 fimbriae in Δ*mfa3*. (A) Sodium dodecyl sulfate–polyacrylamide gel electrophoresis (SDS–PAGE) and Coomassie brilliant blue (CBB) stain of Mfa1 fimbriae from JI-1 and Δ*mfa3*: lane 1, Mfa1 fimbriae from JI-1; lane 2, Mfa1 fimbriae from Δ*mfa3*; lane 3, molecular mass marker. (B) Western blot analysis using α-PGN0290: lane 1, Mfa1 fimbriae from JI-1; lane 2, Mfa1 fimbriae from Δ*mfa3*. (C) Western blot analysis using α-PGN0291: lane 1, Mfa1 fimbriae from JI-1; lane 2, Mfa1 fimbriae from Δ*mfa3*.

Δ*mfa3* shows strong auto-aggregation

Porphyromonas gingivalis cells have a strong ability to auto-aggregate, and deletion of Mfa1 fimbriae was reported to significantly enhance auto-aggregation (Hamada *et al.*, 1996; Kuboniwa *et al.*, 2009). We examined the effect of deletion of *mfa3* on auto-aggregation. The decline in relative OD_{660} value, as a measure of auto-aggregation for the wild-type, was rapid over 20–40 min, reaching 38% at 60 min. In contrast the value for JI-1 (Δ*fimA*) decreased much more slowly, reaching only 60% at 60 min (Fig. 7A). These results confirmed a previous report (Nishiyama *et al.*, 2007). However, the OD_{660} value for the double mutant, SMF-fimA (Δ*fimA* and Δ*mfa1*) decreased much faster than the wild-type, finally reaching 25% of the initial value, suggesting that Mfa1 fimbriae strongly suppress auto-aggregation. Interestingly, the *mfa3* mutant, which still produces Mfa1 fimbriae, showed strong auto-aggregation similar to SMF-fimA, indicating the importance of the accessory components (Mfa3, PGN0290 and PGN0291) in auto-aggregation.

Role of Mfa3 in biofilm formation

Next, biofilm formation of the strains was assessed by the crystal violet method, because auto-aggregation has been reported to play an important role in biofilm formation (Kolenbrander *et al.*, 2006). Consistent with the auto-aggregation results, SMF-fimA and Δ*mfa3* carrying Mfa1 fimbriae without the accessory components demonstrated robust biofilm formation (Fig. 7B). The complementary strain c*mfa3* recovering intact Mfa1, but lacking FimA fimbriae, showed decreased amounts of biofilm formation equivalent to those of JI-1 (Δ*fimA*). Microscopic observation of the biofilms also revealed similar biofilm formation between complemented c*mfa3* and JI-1 (Fig. 7C), again indicating that Mfa1 fimbriae interfere with or regulate the biofilm formation.

DISCUSSION

Gram-negative bacteria express a variety of fimbriae or pili on their cell surface (Fronzes *et al.*, 2008). In pathogenic bacteria these structures are often important virulence factors, mediating biofilm formation, along with attachment to, and invasion of, target

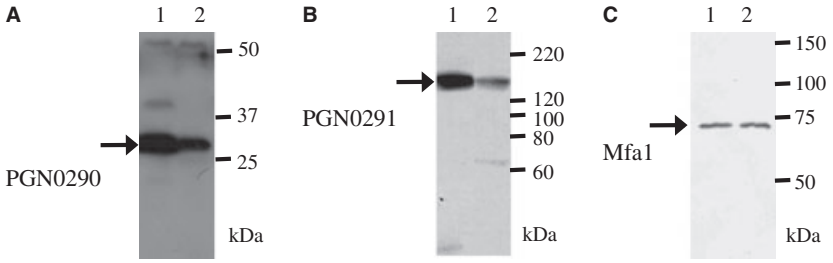

Figure 5 Western blot analysis of PGN0290, PGN0291 and Mfa1 proteins using whole cell lysate and α-PGN0290 (A), α-PGN0291 (B) or chicken α-Mfa1 (C). Lane 1, JI-1; lane 2, Δ*mfa3*.

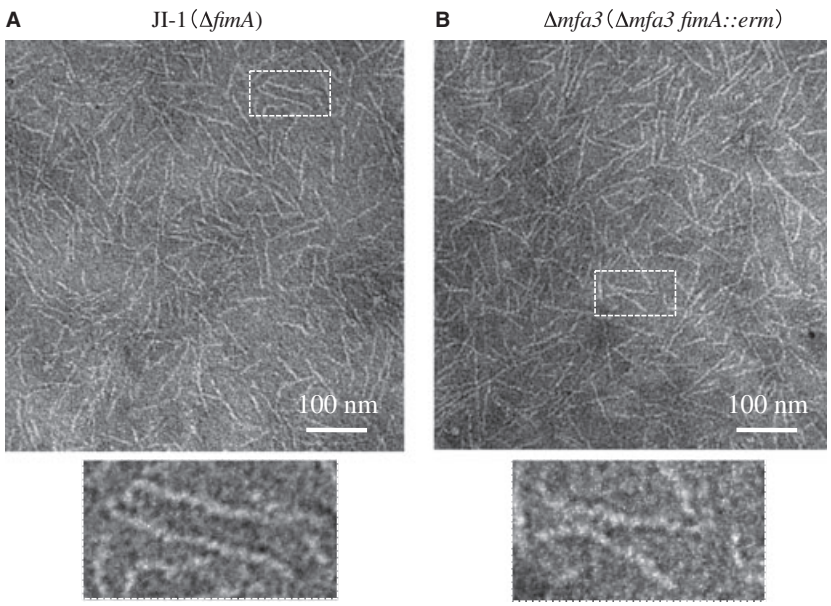

Figure 6 Electron micrographs of the purified Mfa1 fimbriae. Mfa1 fimbriae from JI-1 (A) or Δ*mfa3* (B) were negatively stained with 1% ammonium molybdate. Scale bars indicate the length of 100 nm. The dashed boxes indicate the magnified region shown in the lower panels.

cells (Thanassi *et al.*, 2012). *Porphyromonas gingivalis*, a major pathogen associated with chronic periodontitis, has at least two distinct fimbriae comprised by FimA and Mfa1 structural subunit proteins. Although both fimbriae have several minor proteins as accessory components (Nishiyama *et al.*, 2007; Hasegawa *et al.*, 2009), their exact localization on the fimbrial structure, assembly mechanisms and functions are still unclear. In this study, we show that Mfa3 is produced and transported to the inner membrane as a 43-kDa precursor, then processed and incorporated into Mfa1 fimbrial filaments as an accessory component of 40-kDa (Figs 1C and 2). Incorporated Mfa3 appeared to be at the tip (distal end) of the filaments, based on results of bacterial aggregation (see Fig. S1) and on observations of immune-electron microscopy (Fig. 3). Additionally, in Δ*mfa3*, PGN0290 and PGN0291 were produced and detected in whole cell lysates (Fig. 5A,B), but they were not incorporated into fimbriae (Fig. 4), suggesting that Mfa3 could be required for the assembly of a tip complex consisting of Mfa3, PGN0290 and PGN0291, one or more of which might serve as adhesin(s). Although the expression level of Mfa1 protein and the structure of the purified Mfa1 fimbriae were not changed between Δ*mfa3* and JI-1 (Figs 5C and 6), auto-aggregation and biofilm formation of Δ*mfa3*, similar to those of a double mutant of *mfa1* and *fimA* genes, were enhanced, when compared with JI-1 (Fig. 7). These results suggested that the putative tip complexes are important for fimbrial function.

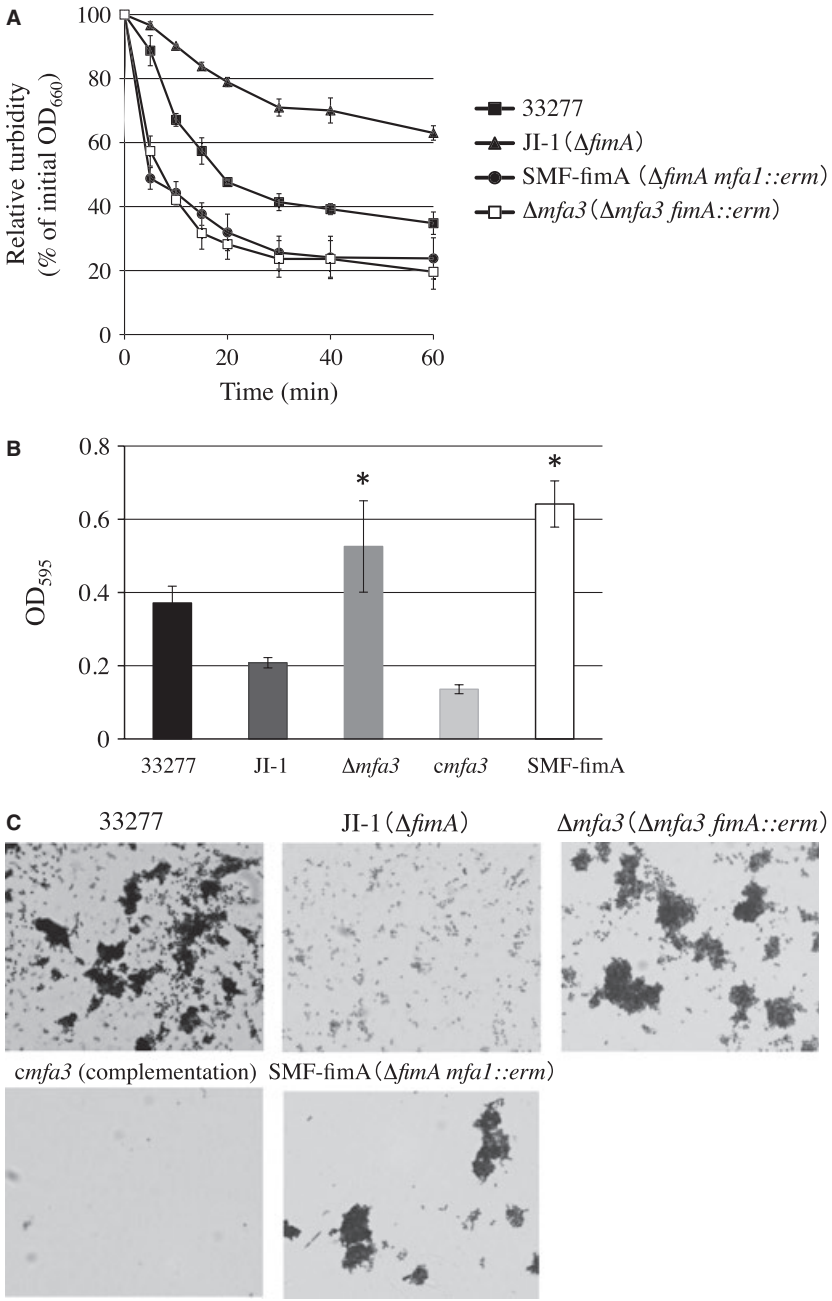

Figure 7 Aggregative phenotype of Δ*mfa3*. (A) Auto-aggregation activities of wild-type (■), JI-1 (▲), SMF-1-fimA (●) and Δ*mfa3* (□). The optical density at 600 nm (OD_{660}) of each cell suspension was measured at the indicated times. Relative turbidities, defined as the relative OD_{660} values (in %) normalized to the initial value of each suspension, are plotted against incubation time. All assays were performed in triplicate and the means ± SD are shown. (B) Biofilm formation by 33277, JI-1, Δ*mfa3*, c*mfa3* and SMF-fimA. The amount of biofilm was quantified by measuring OD_{595} after crystal violet staining and ethanol elution. Data represent the means ± SD ($n = 3$). *Significantly different compared with JI-1, at $P < 0.01$ (Dunnett's test). (C) Microscopic observation. Biofilm structures stained with crystal violet were visualized.

The Mfa3 protein was present in two different sizes of 40 kDa and 43 kDa in the whole cell lysate (Fig. 2). The 43-kDa and 40-kDa Mfa3 were detected largely in the inner membrane and the outer membrane, respectively. The purified Mfa1 fimbriae contained the 40-kDa Mfa3 alone (Fig. 2). Additionally, the N-terminal sequence of the 40-kDa protein was determined as AAHTNGE. This sequence

corresponds to the Ala^{44} residue of the deduced amino acid sequence, suggesting that the 40-kDa Mfa3 protein is produced by cleavage of the Arg^{43}-Ala^{44} bond at the outer membrane. Although the maturation process of the accessory proteins in fimbriae of *P. gingivalis* is not fully understood, it is proposed that the major fimbrilins of FimA and Mfa1 proteins are processed by Rgp and signal peptidase II. The precursor forms of fimbrilins are transported from the cytoplasm to periplasm via the general secretion pathway, and then they are cleaved immediately at the N-terminal side of the cysteine residue by signal peptidase II and transported to the outer membrane (Shoji *et al*., 2004), where FimA and Mfa1 are further processed at amino-acid positions 46 and 49 by Rgp to yield the mature forms, respectively (Nakayama *et al*., 1996; Kadowaki *et al*., 1998). In this study we showed that the N-terminus of mature form of Mfa3 started at Ala^{44} immediately C-terminal to arginine residue, indicating that Rgp is likely to be involved in maturation of the Mfa3 protein. Additionally, we performed LipoP analysis (www.cbs.dtu.dk/services/LipoP/) to predict the cleavage site of the Mfa3 protein by signal peptidases. Mfa3 protein was predicted to have signal peptidase II cleavage sites between the Gly^{20} and Cys^{21} residues (Fig. 1D). These findings raise the possibility that the primary translated form of the Mfa3 accessory protein as well as major fimbrilins are commonly processed. We are presently making an attempt to determine whether Rgp and signal peptidase II are involved in maturation of the accessory protein of Mfa3.

Electron microscopy of the purified Mfa1 fimbriae from parental and Mfa3 mutant strains did not reveal a morphological difference. Hence, Mfa3 seems to be unnecessary for production and polymerization of Mfa1 fimbrilin protein. However, the mechanism of production and polymerization of the Mfa1 protein remains unsolved. In contrast, polymerization of the FimA protein has been partially demonstrated. Previous studies showed that in the absence of FimC–E, FimA protein was produced and polymerized to form the fimbrial structure (Nishiyama *et al*., 2007; Wang *et al*., 2007). Shoji *et al.* (2010) reported that the preproprotein-type recombinant FimA expressed in *E. coli* has the ability to assemble and polymerize to form a filamentous structure in the absence of accessory proteins. Moreover, a very recent study reported a *P. gingivalis* mutant lacking the *fim* cluster, in which *fimA* alone was expressed, exhibiting a fimbrial structure (Nagano *et al*., 2012). This result suggests that the accessory proteins FimC, FimD and FimE are not essential for the polymerization of FimA fimbriae.

Previous studies showed that loss of the Mfa1 fimbriae enhanced auto-aggregation, suggesting that Mfa1 fimbriae might suppress auto-aggregation (Hamada *et al*., 1996; Kuboniwa *et al*., 2009). In contrast, other studies have reported that the Mfa1 fimbriae promoted bacterial auto-aggregation (Lin *et al*., 2006). In the present study, SMF-fimA (Δ*fimA mfa1*::erm) increased auto-aggregation activity compared with JI-1 and 33277 (Fig. 7A), supporting the hypothesis that Mfa1 fimbriae have a suppressive effect on auto-aggregation. Additionally, we have also shown that Δ*mfa3* has an aggregative phenotype similar to SMF1-fimA (Fig. 7A). The significant change of auto-aggregation efficiencies in Δ*mfa3* and SMF-fimA were found to be positively associated with alteration of biofilm structures (Fig. 7B,C). These results suggested that the putative tip accessory proteins of Mfa1 fimbriae are important in the control of homotypic biofilm formation by *P. gingivalis*.

In summary, we have identified Mfa3 as an accessory protein of the Mfa1 fimbriae which is located at the tip of the fimbrial shaft. We have also found that Mfa3 is necessary for the integration of PGN0290 and PGN0291 into the mature fimbrial structure. Although the biological importance of Mfa3 remains to be elucidated, tip proteins positioned away from the cell surface might function in the initial interaction with the human cells or with other bacteria. Future investigation of the structure and functions of Mfa3 as well as other accessory proteins will provide insights into the interactions between Mfa1 fimbriae and the host.

ACKNOWLEDGEMENTS

We thank T. Hirose (Center for Instrumental Analysis, Hokkaido University) for analyzing the amino acid sequence, Y. Hotta (Central Research Laboratories, Asahi University) for performing electron microscopy, and M. Sato (Department of Microbiology, Aichi Gakuin University) for analyzing the mass spectrometry. We also thank the Los Alamos National Laboratory for making the *P. gingivalis* genomic sequence data freely available to the public. This work was supported by Grants-in-Aid for Scientific Research (22791783

and 25861752 to Y.H., 23592720 to Y.M., 23592721 to Y.Y.) from the Japan Society for the Promotion of Science, and DE12505 from the NIH to RJL.

REFERENCES

Abe, T., Murakami, Y., Nagano, K. *et al.* (2011) OmpA-like protein influences cell shape and adhesive activity of *Tannerella forsythia*. *Mol Oral Microbiol* **26**: 374–387.

Amano, A. (2010) Bacterial adhesins to host components in periodontitis. *Periodontol 2000* **52**: 12–37.

Amano, A., Nakagawa, I., Okahashi, N. and Hamada, N. (2004) Variations of *Porphyromonas gingivalis* fimbriae in relation to microbial pathogenesis. *J Periodontal Res* **39**: 136–142.

Daep, C.A., Lamont, R.J. and Demuth, D.R. (2008) Interaction of *Porphyromonas gingivalis* with oral Streptococci requires a motif that resembles the eukaryotic nuclear receptor box protein-protein interaction domain. *Infect Immun* **76**: 3273–3280.

Dickinson, D.P., Kubiniec, M.A., Yoshimura, F. and Genco, R.J. (1988) Molecular cloning and sequencing of the gene encoding the fimbrial subunit protein of *Bacteroides gingivalis*. *J Bacteriol* **170**: 1658–1665.

Fletcher, H.M., Schenkein, H.A., Morgan, R.M., Bailey, K.A., Berry, C.R. and Macrina, F.L. (1995) Virulence of a *Porphyromonas gingivalis* W83 mutant defective in the *prtH* gene. *Infect Immun* **63**: 1521–1528.

Fronzes, R., Remaut, H. and Waksman, G. (2008) Architectures and biogenesis of non-flagellar protein appendages in Gram-negative bacteria. *EMBO J* **27**: 2271–2280.

Gardner, R.G., Russell, J.B., Wilson, D.B., Wang, G.R. and Shoemaker, N.B. (1996) Use of a modified *Bacteroides–Prevotella* shuttle vector to transfer a reconstructed B-1,4-D-endoglucanase gene into *Bacteroides uniformis* and *Prevotella ruminicola* B(1)4. *Appl Environ Microbiol* **62**: 196–202.

Hajishengallis, G., Wang, M., Liang, S. *et al.* (2008) Subversion of innate immunity by periodontopathic bacteria via exploitation of complement receptor-3. *Adv Exp Med Biol* **632**: 203–219.

Hamada, N., Sojar, H.T., Cho, M.I. and Genco, R.J. (1996) Isolation and characterization of a minor fimbria from *Porphyromonas gingivalis*. *Infect Immun* **64**: 4788–4794.

Hasegawa, Y., Iwami, J., Sato, K. *et al.* (2009) Anchoring and length regulation of *Porphyromonas gingivalis* Mfa1 fimbriae by the downstream gene product Mfa2. *Microbiology* **155**: 3333–3347.

Imamura, T., Travis, J. and Potempa, J. (2003) The biphasic virulence activities of gingipains: activation and inactivation of host proteins. *Curr Protein Pept Sci* **4**: 443–450.

Kadowaki, T., Nakayama, K., Yoshimura, F., Okamoto, K., Abe, N. and Yamamoto, K. (1998) Arg-gingipain acts as a major processing enzyme for various cell surface proteins in *Porphyromonas gingivalis*. *J Biol Chem* **273**: 29072–29076.

Kishi, M., Hasegawa, Y., Nagano, K., Nakamura, H., Murakami, Y. and Yoshimura, F. (2012) Identification and characterization of novel glycoproteins involved in growth and biofilm formation by *Porphyromonas gingivalis*. *Mol Oral Microbiol* **27**: 458–470.

Kolenbrander, P.E., Palmer, R.J. Jr, Rickard, A.H., Jakubovics, N.S., Chalmers, N.I. and Diaz, P.I. (2006) Bacterial interactions and successions during plaque development. *Periodontol 2000* **42**: 47–79.

Kuboniwa, M., Amano, A., Hashino, E. *et al.* (2009) Distinct roles of long/short fimbriae and gingipains in homotypic biofilm development by *Porphyromonas gingivalis*. *BMC Microbiol* **9**: 105.

Lamont, R.J. and Jenkinson, H.F. (1998) Life below the gum line: pathogenic mechanisms of *Porphyromonas gingivalis*. *Microbiol Mol Biol Rev* **62**: 1244–1263.

Lamont, R.J. and Jenkinson, H.F. (2000) Subgingival colonization by *Porphyromonas gingivalis*. *Oral Microbiol Immunol* **15**: 341–349.

Lin, X., Wu, J. and Xie, H. (2006) *Porphyromonas gingivalis* minor fimbriae are required for cell–cell interactions. *Infect Immun* **74**: 6011–6015.

Maeda, K., Nagata, H., Kuboniwa, M. *et al.* (2004) Characterization of binding of *Streptococcus oralis* glyceraldehyde-3-phosphate dehydrogenase to *Porphyromonas gingivalis* major fimbriae. *Infect Immun* **72**: 5475–5477.

Murakami, Y., Imai, M., Nakamura, H. and Yoshimura, F. (2002) Separation of the outer membrane and identification of major outer membrane proteins from *Porphyromonas gingivalis*. *Eur J Oral Sci* **110**: 157–162.

Nagano, K., Murakami, Y., Nishikawa, K., Sakakibara, J., Shimozato, K. and Yoshimura, F. (2007) Characterization of RagA and RagB in *Porphyromonas gingivalis*: study using gene-deletion mutants. *J Med Microbiol* **56**: 1536–1548.

Nagano, K., Hasegawa, Y., Murakami, Y., Nishiyama, S. and Yoshimura, F. (2010) FimB regulates FimA fimbriation in *Porphyromonas gingivalis*. *J Dent Res* **89**: 903–908.

Nagano, K., Hasegawa, Y., Abiko, Y., Yoshida, Y., Murakami, Y. and Yoshimura, F. (2012) *Porphyromonas gingivalis* FimA fimbriae: fimbrial assembly by *fimA* alone in the *fim* gene cluster and differential antigenicity among *fimA* genotypes. *PLoS One* **7**: e43722.

Naito, M., Hirakawa, H., Yamashita, A. *et al.* (2008) Determination of the genome sequence of *Porphyromonas gingivalis* strain ATCC 33277 and genomic comparison with strain W83 revealed extensive genome rearrangements in *P. gingivalis*. *DNA Res* **15**: 215–225.

Nakayama, K., Yoshimura, F., Kadowaki, T. and Yamamoto, K. (1996) Involvement of arginine-specific cysteine proteinase (Arg-gingipain) in fimbriation of *Porphyromonas gingivalis*. *J Bacteriol* **178**: 2818–2824.

Nishiyama, S., Murakami, Y., Nagata, H., Shizukuishi, S., Kawagishi, I. and Yoshimura, F. (2007) Involvement of minor components associated with the FimA fimbriae of *Porphyromonas gingivalis* in adhesive functions. *Microbiology* **153**: 1916–1925.

Park, Y., Simionato, M.R., Sekiya, K. *et al.* (2005) Short fimbriae of *Porphyromonas gingivalis* and their role in coadhesion with *Streptococcus gordonii*. *Infect Immun* **73**: 3983–3989.

Pihlstrom, B.L., Michalowicz, B.S. and Johnson, N.W. (2005) Periodontal diseases. *Lancet* **366**: 1809–1820.

Proft, T. and Baker, E.N. (2009) Pili in Gram-negative and Gram-positive bacteria – structure, assembly and their role in disease. *Cell Mol Life Sci* **66**: 613–635.

Shoji, M., Naito, M., Yukitake, H. *et al.* (2004) The major structural components of two cell surface filaments of *Porphyromonas gingivalis* are matured through lipoprotein precursors. *Mol Microbiol* **52**: 1513–1525.

Shoji, M., Yoshimura, A., Yoshioka, H. *et al.* (2010) Recombinant *Porphyromonas gingivalis* FimA preproprotein expressed in *Escherichia coli* is lipidated and the mature or processed recombinant FimA protein forms a short filament *in vitro*. *Can J Microbiol* **56**: 959–967.

Thanassi, D.G., Bliska, J.B. and Christie, P.J. (2012) Surface organelles assembled by secretion systems of Gram-negative bacteria: diversity in structure and function. *FEMS Microbiol Rev* **36**: 1046–1082.

Wang, M., Shakhatreh, M.A., James, D. *et al.* (2007) Fimbrial proteins of *Porphyromonas gingivalis* mediate *in vivo* virulence and exploit TLR2 and complement receptor 3 to persist in macrophages. *J Immunol* **179**: 2349–2358.

Watanabe, K., Onoe, T., Ozeki, M. *et al.* (1996) Sequence and product analyses of the four genes downstream from the fimbrilin gene (*fimA*) of the oral anaerobe *Porphyromonas gingivalis*. *Microbiol Immunol* **40**: 725–734.

Watanabe-Kato, T., Hayashi, J.I., Terazawa, Y. *et al.* (1998) Isolation and characterization of transposon-induced mutants of *Porphyromonas gingivalis* deficient in fimbriation. *Microb Pathog* **24**: 25–35.

Yilmaz, O., Watanabe, K. and Lamont, R.J. (2002) Involvement of integrins in fimbriae-mediated binding and invasion by *Porphyromonas gingivalis*. *Cell Microbiol* **4**: 305–314.

Yoshimura, F., Murakami, Y., Nishikawa, K., Hasegawa, Y. and Kawaminami, S. (2009) Surface components of *Porphyromonas gingivalis*. *J Periodontal Res* **44**: 1–12.

SUPPORTING INFORMATION

Additional Supporting Information may be found in the online version of this article:

Figure S1. Bacterial aggregation using recombinant accessory protein-specific antiserum.